https://doi.org/10.5194/egusphere-2026-1689
Preprint. Discussion started: 31 March 2026

Why multitemporal ALS forest metrics remain challenging: Insights from operational airborne laser scanning

Charis Moana Gretler[a, *], Daniel Kükenbrink[a, *], Mauro Marty[a], Christian Ginzler[a], Felix Morsdorf[b]

[a] Landchange Science, Swiss Federal Institute WSL, Zürcherstrasse 111, Birmensdorf, CH-8903, Switzerland
[b] Remote Sensing Laboratories, Department of Geography, University of Zurich, CH-8057 Zurich, Switzerland

[*] *Correspondence to:* Charis Moana Gretler (charis.gretler@wsl.ch) and Daniel Kükenbrink (daniel.kuekenbrink@wsl.ch)

https://doi.org/10.5194/egusphere-2026-1689
Preprint. Discussion started: 31 March 2026

Abstract

The increasing availability of large-scale and repeated operational airborne laser scanning (ALS) facilitates its use for multitemporal analyses and monitoring. In the last decades, single ALS acquisitions have been demonstrated to hold great potential for obtaining forest structural information. However, the robustness and reliability of ALS to accurately detect changes in complex forest structural parameters such as plant area index (PAI), from repeated ALS acquisitions have rarely been assessed. In this study, we evaluated the reliability and limitations of multitemporal mapping and interpretation of this structural trait, using the well-established canopy height (CH) as a reference metric. We used operational ALS data from a heterogeneous temperate forest in northern Switzerland from three years, 2014, 2019 and 2020, recorded with different sensor and flight settings. Our results showed that CH was largely unaffected by the differences in data acquisition, reaffirming it to be a robust trait and demonstrating that our data is usable for multitemporal analyses. For PAI, we applied and compared three estimation methods with varying complexity. PAI results were highly sensitive to various acquisition parameters, particularly the pulse repetition frequency, leading to large deviations between acquisitions. All tested PAI estimation methods exhibited similar problems, complicating the distinction between actual structural change and external effects. This study underscores the potential of operational ALS for multitemporal forest structure analyses but highlights the need for standardisation of recording parameters as much as possible, as well as methodological harmonization and calibration to ensure comparability in multitemporal analyses, particularly for complex forest structural traits.

Keywords: ALS, canopy height, forest structure, LiDAR, multitemporal, PAI, vegetation density

https://doi.org/10.5194/egusphere-2026-1689
Preprint. Discussion started: 31 March 2026

1 Introduction

The increasing availability of airborne laser scanning (ALS) data over the past decades has created new opportunities for analysing forest structure across large areas. Structural forest attributes derived from ALS, such as canopy height, volume and biomass provide valuable insights into forest development, productivity and ecological function (Homolová et al., 2013; Riofrío et al., 2022; Schneider et al., 2017). In the context of global change—including climate impacts and increasing anthropogenic pressures—monitoring forest structure has become essential for understanding and managing these systems. Forests not only fulfil important ecosystem services and provide protective and utility functions but also act as biodiversity hotspots and crucial carbon sinks, making them critical to conservation efforts (Bonan, 2008). Among the key dimensions of forest ecosystems are composition, structure and function (McElhinny et al., 2005; Noss, 1990). While compositional and structural characteristics have traditionally formed the basis of forest inventories, functional aspects have gained increasing attention in recent years (e.g. Helfenstein et al., 2022; Schneider et al., 2017; Zheng et al., 2021). Plant functional traits have been demonstrated to show a positive relationship between plant diversity and ecosystem functioning (Schneider et al., 2017). Such traits can be of morphological, physiological or phenological nature (Helfenstein et al., 2022; Homolová et al., 2013). Morphological traits are linked to the availability of light and other factors, such as the growth rate of individual trees, the productivity of the ecosystem, and the specific habitat for canopy-dwelling organisms (Ishii et al., 2004; Moles et al., 2009; Zheng et al., 2021). Canopy height (CH) and plant area index (PAI) are examples of morphological forest traits. These two traits represent different aspects of canopy structure—vertical extent and canopy openness—and thus reflect key dimensions of forest architecture (Fahey et al., 2019).

CH is widely used in ecological and forestry studies as an indicator of stand development, biomass and productivity. It has been shown to play a central role in plant ecological strategies, as it determines how well a plant can compete for light, which affects the carbon gain strategy of a species (Moles et al., 2009; Stahl et al., 2014). Furthermore, CH has been related to various species' abundances (Coops et al., 2016). For CH, there is a robust body of literature demonstrating reliable retrieval from ALS data and ecological interpretation (Coops et al., 2016; Fischer et al., 2024; Pearse et al., 2019; Tompalski et al., 2019; Wilkes et al., 2015). It can robustly and easily be estimated from ALS data and serves as a standard metric in many structural analyses. In contrast, PAI – defined as half the total surface area of all plant material (leaves and woody structures) per unit ground area (Chen et al., 1991) – is more complex to estimate. In forests, PAI is often estimated rather than leaf area index (LAI), due to the existence of woody structures (Liu et al., 2021; Solberg et al., 2009). LAI, a much-studied variable, is considered an important climate and biodiversity variable, as it influences photosynthesis, transpiration and rain interception (Bojinski et al., 2014; Liu et al., 2021; Skidmore et al., 2015). Although passive sensors and synthetic aperture radar (SAR) have been used to estimate LAI and PAI, respectively, they are subject to limitations such as saturation at high trait values, shading, variable moisture conditions, or ground and terrain effects (Solberg et al., 2009). ALS has shown promising results and offers methods for estimating PAI through the Beer–Lambert law (Arnqvist et al., 2020). Additionally, with ALS it is possible to constrain PAI estimation to specific vertical layers of the canopy using height thresholds (Morsdorf et al., 2006). This allows researchers to isolate canopy-level PAI from total vegetation density – an approach not feasible with passive sensors, which typically integrate signals over the full vertical profile. Such layer-specific analysis is particularly useful for understanding forest structure dynamics and canopy openness, especially under leaf-off conditions when understorey and overstorey can be more clearly separated.

Spatial continuous trait mapping, enabled by ALS, can fill existing data gaps. Beyond single-date trait estimation, the rising availability of repeated ALS acquisitions now facilitates multitemporal analyses of forest structure. Studies in this field have largely focused on CH change as a proxy for tree growth (e.g. Kozniewski et al., 2022; Tymińska-Czabańska et al., 2022; PinYu et al., 2005) or disturbances. Some researchers have also examined changes in canopy cover or vertical echo distribution using the complete 3D point clouds (Arumäe et al., 2020; Leiterer et al., 2015a). However, most physically based (Hyyppä et al., 2008) multitemporal ALS studies to date have been limited to height metrics, and relatively few have addressed how

https://doi.org/10.5194/egusphere-2026-1689
Preprint. Discussion started: 31 March 2026

complex structural traits, such as vegetation density, change over time. In a multitemporal analysis of vegetation structure beyond height metrics, Shao et al. (2019) examined ALS survey pairs over Amazon forests and demonstrated that sensor differences and varying pulse densities can introduce systematic biases in structural change estimates, and the authors proposed a correction based on linear regression.

Many multitemporal ALS studies to date rely on data acquired specifically for research purposes, often using comparable sensor configurations and harmonized acquisition settings. In contrast, operational ALS datasets, such as those increasingly available from national or regional mapping programs, are typically collected over long time periods using different sensors, flight geometries and acquisition parameters. These heterogeneous conditions—e.g. varying flight altitudes, beam divergences, scan angles, pulse repetition frequencies, and footprint sizes—can substantially influence the derived parameters, probably affecting the robustness of multitemporal trait estimations (Morsdorf et al., 2008; Næsset, 2009; Ørka et al., 2010; Solberg et al., 2009). Such variability could introduce substantial confounding effects and complicate a clear attribution of temporal differences to ecological processes.

Consequently, a notable research gap becomes apparent: despite the growing availability of operational ALS data across large regions and multiple points in time, the temporal dynamics of complex morphological traits—such as PAI— using operational ALS acquisitions from national or large scale surveys have rarely been analysed. Most existing studies rely on harmonized research datasets or examine forests that differ fundamentally from temperate systems, such as tropical Amazonian forests, whose structural and phenological characteristics are not directly transferable to temperate forest systems (e.g. Shao et al., 2019). As a result, it remains unclear how reliably complex traits can be mapped over time using operational, non-standardized data in temperate forests. Addressing this gap is essential, as operational ALS time series have the potential to support large-scale monitoring of forest structure relevant to ecosystem function, biodiversity, and evidence-based forest management. Yet their suitability for deriving consistent multitemporal trait information remains largely unexplored.

The main objective of this paper is to evaluate the reliability and limitations of multitemporal mapping of morphological forest traits using operational ALS data. In this study, we therefore introduce CH as a baseline metric—one that is well understood and relatively insensitive to acquisition differences. This baseline allows us to contextualize our main focus: assessing PAI, a trait that is far more susceptible to variations in sensor and flight parameters. By contrasting these two traits, we aim to highlight a critical yet often overlooked issue in multitemporal ALS analyses and stimulate a broader discussion on the reliability of complex structural metrics from ALS data. We use data from three operational ALS acquisitions (2014, 2019, 2020) across a large, forested area in the western part of the canton of Aargau, Switzerland. Our aim is to highlight critical sources of uncertainty and to raise awareness of the methodological constraints that accompany the use of operational multitemporal ALS for trait-based forest monitoring.

The following research questions guide our work:

- How consistent and reliable are CH and PAI estimates derived from ALS across different acquisition years and forest types?
- How do differences in sensor and flight parameters affect the comparability of structural trait estimates, particularly for complex density-based metrics such as PAI?
- Which ALS-based PAI-estimation method provides the most consistent and interpretable results over time?

Rather than proposing a correction approach, our objective is to identify and quantify acquisition-related effects that can confound the interpretation of multitemporal ALS-derived forest metrics.

https://doi.org/10.5194/egusphere-2026-1689
Preprint. Discussion started: 31 March 2026

2 Material and methods

2.1 Airborne laser scanning data

For the years 2014 and 2019, two ALS datasets containing the entire area of the canton Aargau were made available by their local government (Departement Bau, Verkehr und Umwelt, Abteilung Wald) in the reference system LV95/LN02 (EPSG:2056/5728). The data from 2014 were acquired under leaf-off (defoliated) conditions. The data were collected from 18.03.2014 to 04.04.2014 with an LMS-Q680i RIEGL scanner. In 2019, leaf-off data were collected from 23.03.2019 to 21.04.2019 with an LMS-VQ780i RIEGL scanner. The aerial surveys in 2014 and 2019 were carried out by Milan Geoservice GmbH (Kamenz, Germany).

For the year 2020, an ALS dataset covering the entire canton of Aargau, acquired as part of the swissSURFACE^{3D} product, was provided by the Federal Office of Topography swisstopo. The leaf-off data were acquired from 06.02.2020 to 14.03.2020. The acquisitions mostly took place during the night and were done with various aeroplanes using a Riegl VQ-780i and a Riegl LMS-Q780 scanner. More details about the data used in this study can be found in Table 1.

Table 1. Summary of the specifications for airborne laser scanning (ALS) data acquisitions in the canton of Aargau in 2014, 2019 and 2020.

	2014 (leaf-off)	2019 (leaf-off)	2020 (leaf-off)
Acquisition date	18.3.-4.4.2014	23.3.-21.4.2019	6.2-14.3.2020
Flight trajectory available?	✓	✓	✓
ALS sensor	LMS-Q680i	LMS-VQ780i	Riegl VQ-780i & Riegl LMS-Q780
Mean operating altitude above ground [m]	600	1250	1275
Scan angle [°]	±15	±30	±30
Mean point density [pts/m^2]	16	30.8	17.5
Pulse footprint at mean operating altitude [cm]	30	31	32
Pulse repetition frequency [kHz]	300	1000	VQ780i: 500 / Q780: 400
Beam divergence [mrad]	0.5	0.25	0.25
Laser wavelength	NIR	NIR	NIR

For most computations the ALS data had to be terrain-normalized (CH, PAI using leafR and Arnqvist approaches, see Sect.s 2.3.2 and 2.3.3). This means that information on the z-values of all points was converted from metres above sea level to metres above ground level, by calculating their height above the ground surface (points classified as ground). The “lasheight” tool from the LAStools software package was used for this task (Isenburg, 2022).

2.2 Study area

Our study area is located in the western part of the canton of Aargau in northern Switzerland. It covers 361 km^2, around 40% of the area is covered by forests. The site has a variety of forest types and is subject to different forest management practices (Leiterer et al., 2015b). Terrain height varies from 260 to 980 m a.s.l.

https://doi.org/10.5194/egusphere-2026-1689
Preprint. Discussion started: 31 March 2026

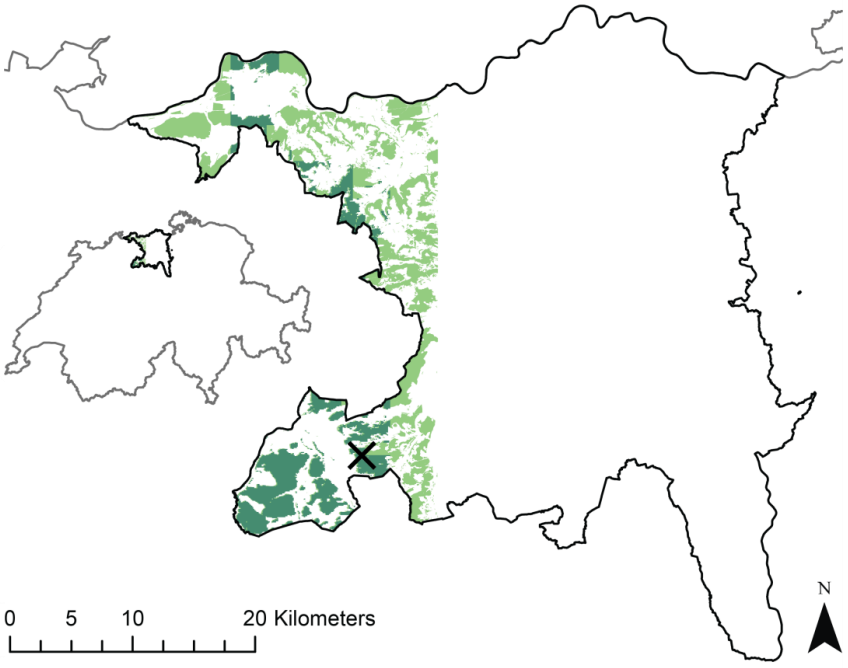

Figure 1. Overview of the study area in greens (right) and its location in Switzerland (left) (Federal Office of Topography swisstopo, 2022a). The full CH analysis area is shown in light and dark green, whereas the PAI analysis area is highlighted in dark green. The black cross marks the location of the scale sensitivity test site (see Table S1 in the Supplementary Material).

Deciduous forests cover approximately 40% of the forested study area, pure coniferous stands account for 15%, and the remaining 45% consists of mixed forest types. Coniferous forests are more prevalent in the southwestern region of the canton of Aargau. The predominant tree species are *Fagus sylvatica*, making up 32% of the forest stand, and *Picea abies* (26%) (Canton Aargau: Departement Bau Verkehr und Umwelt, 2018)

2.2.1 Forest classification

Dominant leaf type may have an influence on the distribution of LiDAR returns in the vegetation. We determined four different forest types using the deciduous tree mix rate provided by Waser and Ginzler (2021): coniferous forest, mixed coniferous forest, mixed deciduous forest, and deciduous forest. The classification follows the classes of the Swiss National Forest Inventory NFI (Table 2).

Table 2: Forest mix rate classification, after Brändli et al. (2020).

Value	Description	Deciduous tree mix rate [%]
1	coniferous forest	0–10
2	mixed coniferous forest	11–50
3	mixed deciduous forest	51–90
4	deciduous forest	91–100

2.2.2 Reference forest area for PAI method comparison

To see how well a given PAI method performed, we compared our PAI outputs from the study area to a reference. This reference needed to be a representative area of forest where little to no change happened during the study years of 2014, 2019 and 2020.

https://doi.org/10.5194/egusphere-2026-1689
Preprint. Discussion started: 31 March 2026

In theory, a perfect method would yield highly consistent results across all three years. Any differences observed in the PAI outputs between years could therefore be attributed either to the method itself or to variations in the input data.

As a completely static reference forest is nearly impossible to find, we searched for forest patches that were expected to show no or only very few changes in forest structure over the period 2014–2020. We expected older coniferous forest patches to fulfil this requirement. The definition of our reference forest is as follows:

1. coniferous forest: deciduous tree mix rate ≤ 10%
2. CH > 30 m (where the CH is defined as the height of 95% of the vertical point distribution per pixel (H95, computed as in Sect. 2.3.2)
3. height difference lower than 0.5 m between 2014 and 2020

Due to this definition, the reference forest does not form a contiguous area but consists of pixels scattered across the forested study area. The result is a binary reference raster grid with a cell size of 2 × 2 m, which was used to compare the outputs of the different methods to estimate PAI.

2.3 Structure metrics

We focused on different traits for the characterization of height and density. Our selected morphological traits relate to two of the three primary components of variation in canopy space: canopy height and openness (Fahey et al., 2019). These structural axes have been linked to ecosystem functioning and are commonly used to differentiate between vegetation types. They have also been used to characterize the structural diversity of the canopy (Coops et al., 2016; Zheng et al., 2021).

2.3.1 Scale sensitivity

As methods to retrieve structural traits are highly sensitive to cell dimensions, we performed a scale sensitivity analysis that further defined the chosen cell size of 2 × 2 × 2 m. We tested cell sizes of 1, 2, 5, 10 and 20 m and conducted the analysis on a specifically selected mixed forest patch of 1.67 km^2 (see Supplementary Material). The patch (47.264° N, 7.960° E) was selected as it contains both deciduous and coniferous stands and provides a representative subset of the forest structures found across the study area.

2.3.2 Height metrics

CH is one of the most common derivatives of ALS data because it is easy to compute and shows high accuracy with less bias compared with field-based measurements (Coops et al., 2016). For this reason, CH was used as a baseline metric in our analysis. Owing to its proven robustness, CH is expected to be largely insensitive to heterogeneity in operational ALS acquisitions. If substantial inconsistencies were observed, this would call into question the overall suitability of the data for multitemporal structural analyses.

For our analysis, we investigated two height metrics, the maximum height (Hmax) and the 95th percentile (H95) per pixel. We derived both Hmax and H95 from the normalized ALS point cloud data on a grid with a resolution of 2 m. For our investigation, we defined Hmax per pixel as the maximum value of the normalized points per pixel.

As a second vegetation height characteristic, we estimated the height of 95% of the vertical point distribution per pixel (H95). This characteristic is used very often, as it is less susceptible to outliers than Hmax. Points below 3 m (NFI definition of the minimum tree height) were not considered, in order to separate the understorey from the canopy.

https://doi.org/10.5194/egusphere-2026-1689
Preprint. Discussion started: 31 March 2026

2.3.3 Density metrics

The estimation of plant area index (PAI) constitutes the main experimental focus of this study. Different approaches to estimate PAI are available, all of which have advantages and disadvantages. We tested three methods, all based on the Beer–Lambert law of light extinction, with increasing complexity level:

- estimation using first returns from de Almeida et al. (2019), implemented in R (leafR package; (de Almeida et al., 2022), adapted to using all returns
- estimation using scaling of intensity values and returns from Arnqvist et al. (2020), implemented in Python
- estimation using ray tracing with the AMAPVox tool developed by Vincent et al. (2017), implemented in R and JAVA

The more complex the method, the more time-consuming and computationally intensive the estimation of PAI. Therefore, the motivation arose to use methods with different complexity levels to be able to compare the derived results and find the optimal method with satisfactory results. The methods are based on a voxel grid and involve estimating the plant area density (PAD) as a first step. PAD is then summed within the vertical voxel column to obtain PAI.

We chose a voxel size of 2 × 2 × 2 m for all methods, resulting in a PAI grid with a resolution of 2 × 2 m (see 4.1 Scale sensitivity). We used the terrain-normalized point clouds for the leafR and Arnqvist methods but the non-normalized point clouds for AMAPVox, as the original ALS data are required for ray tracing.

leafR method

The study by de Almeida et al. (2019) followed the approach of assuming that all laser pulses are vertically aligned. This made it possible to dispense with a complex voxel traversal algorithm, as the movement of the laser pulses was only tracked within the voxel columns. PAI is estimated as follows:

$$PAI = \sum PAD \tag{1}$$

where plant area density (PAD) is the vertical distribution of plant elements in the *i*th canopy layer, estimated by applying the MacArthur–Horn equation:

$$PAD_i = ln\left(\frac{pulses.in_i}{pulses.out_i}\right) \cdot \frac{1}{D_z} \cdot \frac{1}{k} \tag{2}$$

where D_z is the vertical resolution of the canopy layer, $pulses.in_i$ is the number of pulses entering the voxel and $pulses.out_i$ is the number of pulses passing through the voxel. Here, only first returns can be considered because the MacArthur–Horn approach works under the assumption that each pulse represents an independent canopy probe. Therefore, the number of emitted pulses has to be equal to the number of reflections. This leads to a large part of the dataset being disregarded. Furthermore, it is expected to have a high site-to-site variability, due to the method being sensitive to the ratio of the LiDAR footprint and the mean gap size in the canopy. We applied the leafR method to a dataset using all returns and not just the first returns to omit gaps in the resulting map. This alteration represents a simplification of the original theoretical assumptions. The results therefore only serve as a first approximation and are intended to provide an initial impression of the vegetation density. It is also interesting to compare this rather simple estimation method with the more complex methods that are presented below. Arnqvist et al. (2020) did the same in their study and reported that this modification avoided other documented difficulties associated with using only first returns, while still providing an estimate of PAI using a computationally very inexpensive method.

https://doi.org/10.5194/egusphere-2026-1689
Preprint. Discussion started: 31 March 2026

Arnqvist method

Arnqvist et al. (2020) proposed a hybrid method in which they combined two different methods. The first sub-method extends the approach originally developed by de Almeida et al. (2019), which Arnqvist et al. (2020) modified by including the scan angle in their estimation.

The second sub-method is based on the approach of Hopkinson and Chasmer (2009), which relies on the ALS intensity values. This approach assumes that the intensity values depend on the density of the vertical forest section and that the albedo is identical for soil and vegetation (Arnqvist et al., 2020). The main advantage is that all returns are utilized and many disadvantages of the leafR method are mitigated. A disadvantage, however, is the assumption that the albedo of soil and vegetation is identical, which is particularly problematic in less dense forests.

By combining these two methods, the respective strengths could be combined and many of the problems encountered could be solved. The PAI value is estimated in four steps. First, all returns are identified and scaled according to their intensity. The mathematical formula for scaling the individual pulses is as follows:

$$r_s = \frac{I_{i_r}}{\sum_{i_r=1}^{N_r} I_{i_r}}, \tag{3}$$

where r_s is the rescaled intensity of the i_rth return of the pulse, where the original intensity is I_{i_r}. The scaling factor is the sum of all intensities between the first and the maximal return number (N_R) of the pulse. After the intensities are scaled, the approach estimates the ratio of incoming and outgoing radiation in a second step:

$$\frac{\sum_{i=1}^{k} R_i}{\sum_{i=1}^{k+1} R_i} = \frac{\sum_{i=1}^{k} r_{s_i}}{\sum_{i=1}^{k+1} r_{s_i}}, \tag{4}$$

where R is the radiation reflected at height z. Thirdly, it calculates PAD using the following equation:

$$\overline{PAD}\Delta z = -\frac{\cos\theta_1}{\mu} \ln\left(\frac{\sum_{i=1}^{k} R_i}{\sum_{i=1}^{k+1} R_i}\right), \tag{5}$$

where θ_1 is the pulse-specific scanning angle of incoming radiation and μ is the extinction coefficient with a default of $\mu = 0.5$, as a spherical distribution of the reflecting vegetation surfaces is assumed. The PAI is then calculated using Eq. (1) in the last step.

Due to this weighting, the Arnqvist method is either equivalent to the leafR method, in cases where there is a first-return-only dataset, or the Hopkinson and Chasmer (2009) method if only one return over the binning area is available.

AMAPVox

The AMAPVox tool (used Version 1.10.4.) is a JAVA-based implementation that performs ray tracing of each laser pulse (Vincent et al., 2017, 2021). This means that the path of each emitted pulse is traced through a three-dimensional (3D) voxel grid. In addition to the 3D point cloud, this requires the exact position of the sensor at the time of emission. This is stored in the trajectory file.

In AMAPVox, the trajectories are combined with the point clouds. The tool analyzes the extinction of the signal on its path through the voxel grid. This allows the transmission P_{Gap}, i.e. the transmittance (this is the estimator used for this study), to be calculated for each voxel:

https://doi.org/10.5194/egusphere-2026-1689
Preprint. Discussion started: 31 March 2026

$$-\sum_{q}^{N} BFent_q S_q P_{Gap}^{l_q} = \sum_{q}^{N} BFout_q S_q \quad (6)$$

q is the pulse index, N is the number of pulses entering a voxel, S_q is the cross section of pulse q in the center of the voxel, *BFent* and *BFout* are the beam surface fraction at the entrance and exit of the voxel, respectively, and l_q is the potential optical path length of pulse q from the entrance to the expected exit point. P_{Gap} is then converted into an estimate of the plant area density (PAD), where θ is the viewing direction of the beam:

$$PAD = -\frac{\ln(P_{Gap})}{G(\theta)} \quad (7)$$

AMAPVox enables to define various parameters of the sensor so that the calculation is adapted to the respective ALS data. These calculations typically involve high computing costs with large Memory consumption.

2.3.4 Statistical analysis of interannual consistency

To assess the robustness and comparability of ALS–derived structural traits across acquisition years, we applied a combination of paired non-parametric tests and distribution-based comparisons on pixel-wise values. Because the same spatial units (2 × 2 m pixels) were evaluated in each year, all analyses were conducted on paired observations.

Systematic interannual changes in CH and PAI were evaluated using paired Wilcoxon signed-rank tests. This non-parametric approach was chosen to account for the very large sample size, the presence of outliers, and deviations from normality in the pixel-wise differences. Given the sensitivity of p-values to large sample sizes, test results were interpreted primarily based on effect sizes, including median differences and interquartile ranges of the interannual differences.

In addition to assessing changes in central tendency, we evaluated the similarity of the full value distributions between acquisition years using pairwise Kolmogorov–Smirnov (KS) tests. The KS test compares the empirical cumulative distribution functions and thus captures differences in distributional shape, spread, and tails, which are not reflected by location-based tests alone. The KS D statistic was used as the primary measure of distributional similarity, while p-values were considered only in a supportive role.

All statistical analyses were performed separately for CH and for PAI derived from the three different estimation methods, allowing us to distinguish robust structural traits from metrics that are sensitive to acquisition-related effects. We used the R base package stats, under R Version 4.2.3 for all statistical analyses.

https://doi.org/10.5194/egusphere-2026-1689
Preprint. Discussion started: 31 March 2026

3 Results

3.1 Scale sensitivity

The sensitivity analysis (see Sect. 2.3.1) showed different results for the PAI and CH metrics. As is visible in Figure 2 a, b and c, the plots for PAI showed a similar pattern for all the methods considered. Mean PAI increased from 1 to 2 m cell size and then continuously levelled out. The observed variation peaked at a cell size of 2 m and decreased with larger cell sizes.

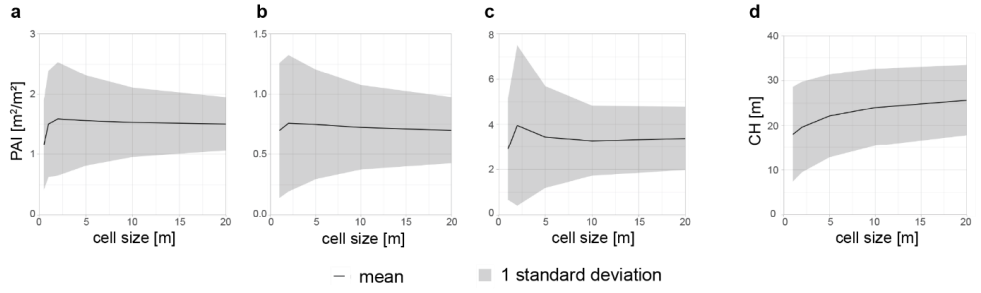

Figure 2. Dependence of the mean and plus/minus one standard deviation of the metrics plant area index (PAI; a: leafR method, b: Arnqvist method, c: AMAPVox method) and canopy height (CH; d: H95) on cell size. Note the different y-axis ranges for each PAI method.

CH followed a different curve, as depicted in Figure 2d. The larger the cell size, the higher the recorded CH. Like in the PAI plots, the variation in CH decreased with larger cell sizes, but this loss of variability was not as pronounced as with PAI.

3.2 Differences in structural traits

3.2.1 Height metrics

Figure 3 shows the estimated CH in all three years for our entire study area. The boxplots and the density diagram show very similar values between the study years. The results for 2019 and 2020 were almost identical, while in 2014 fewer pixels were detected with CH between 8 and 18 m.

Median pixel-wise differences in CH were small for all year pairs, amounting to 0.9–1.1 m between 2014 and the later acquisitions and only 0.13 m between 2019 and 2020 (Table S2). Interquartile ranges of the differences were narrow, particularly for 2019–2020. Pairwise KS tests yielded very small D statistics (< 0.014), confirming a high degree of distributional similarity across all years. Although paired tests were statistically significant due to the large sample size, effect sizes indicate only minor interannual variation in CH.

Between 2014 and 2019/2020, the number of pixels with a CH < 10 m decreased, whereas the number of pixels with a CH of 10 to 20 m increased. Above a CH of 20 m, only minor changes were detected between 2014 and 2019/2020. Only slight changes were seen in areas with a high CH. There were fewer pixels with a CH of 27–34 m in 2020 than in 2014. Areas with a very high CH (> 35 m) did not change, as seen in the overlapping curves in the density plot (Figure 3b). The mean CH over the entire study area decreased very slightly from 2014 (= 21.44 m) to 2019 (= 21.31 m), to 2020 (= 21.26 m).

https://doi.org/10.5194/egusphere-2026-1689
Preprint. Discussion started: 31 March 2026

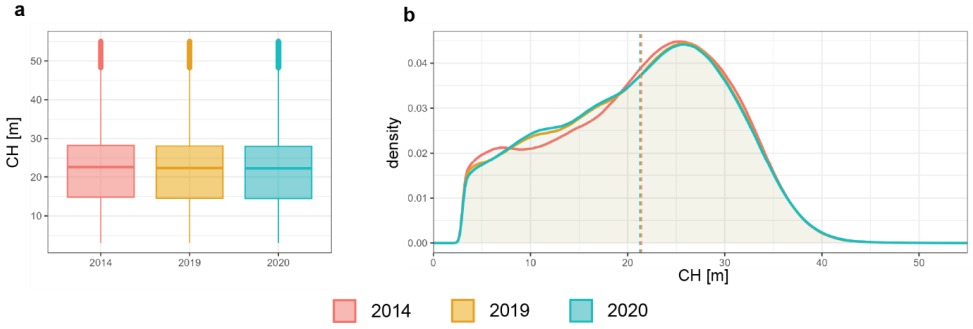

Figure 3. Boxplots (a) and density plots (b) of the estimated canopy height (CH) values of all three study years using the 95th percentile height (H95). The mean values over the entire study area (dashed lines) are 21.44 m in 2014, 21.31 m in 2019, and 21.26 m in 2020.

For CH, the metric Hmax showed the same pattern as H95 but with slightly higher values: mean Hmax is 21.82 m in 2014, slightly higher (22.05 m) in 2019, and then 21.68 m in 2020. Like H95, Hmax decreased between 2014 and 2020, but increased slightly between 2014 and 2019.

3.2.2 Density metrics

We estimated density metrics for the study area in 1000 × 1000 m tiles. Some of these tiles did not run with AMAPVox, due to inconsistencies between the point clouds and the provided trajectories, such as mismatched GPS time information or missing pulse emission records in the trajectories, which impeded the correct association of laser returns with their corresponding sensor positions. We therefore only used the correctly computed tiles that were available from all three methods. This reduced the size of the test area for all density metrics to ~ 56.1 km^2 (Table S1).

The three methods led to very different ranges in PAI (Figure 4). PAI values varied between 0 and 5 for leafR, the simplest method, between 0 and 8 for the Arnqvist method, and between 0 and 18 for the most complex raytracing algorithm, AMAPVox. The respective mean PAI values are shown in Table 3. The methods all resulted in a somewhat similar distribution of the PAI values in the density plots, where the values peaked in the lower half of their ranges and then decreased towards the higher end of their ranges. The high occurrence of very low PAI values was expected, as we did not filter out forest borders and clearings. The exact distributions of the PAI values depended on the method used. For example, the AMAPVox method led to a larger proportion with high PAI values next to the peak compared with the Arnqvist method. The AMAPVox method provided more very dense vegetation voxels compared with the other methods.

Table 3: Mean and standard deviation (sd) of the plant area index (PAI) [m2/m2] from the study years 2014, 2019 and 2020 using all three tested methods.

	2014	**2019**	**2020**
leafR	1.29 (sd = 0.76)	1.04 (sd = 0.76)	1.36 (sd = 0.78)
Arnqvist	2.42 (sd = 1.32)	2.08 (sd = 1.47)	2.64 (sd = 1.38)
AMAPVox	3.35 (sd = 3.09)	3.18 (sd = 3.58)	3.68 (sd = 3.58)

https://doi.org/10.5194/egusphere-2026-1689
Preprint. Discussion started: 31 March 2026

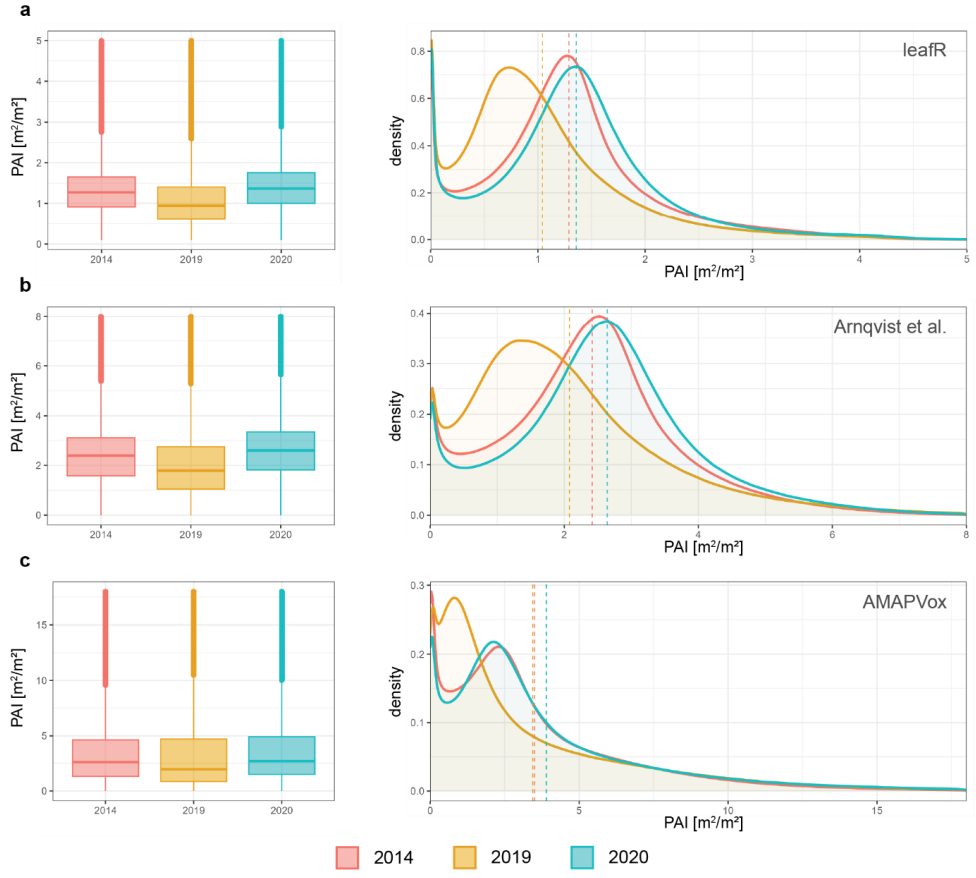

Figure 4. Boxplots (left) and density plots (right) of the estimated plant area index (PAI) values of all three study years using the methods leafR (a), Arnqvist (b) and AMAPVox (c). The dashed vertical lines in the density plots indicate the mean value. The PAI ranges are different for each method.

The differences between the years were much larger for PAI than for the CH estimations. A general pattern was visible in the results of all PAI methods: the peak in the density plot for the years 2014 and 2020 were at a similar PAI value, while the one for 2019 was much lower. The mean PAI values did not represent the similarity of the value distributions for 2014 and 2020. With all PAI methods, 2020 showed the highest and 2019 the lowest mean PAI value, while the value for 2014 was intermediate.

PAI showed substantial interannual variability for all three estimation methods. Paired non-parametric tests indicated systematic differences in pixel-wise PAI values between all acquisition year pairs for the leafR, Arnqvist and AMAPVox approaches (Tables S3-S5). Median differences between years were notably larger than those observed for CH, and the interquartile ranges of the differences were broad for all methods.

Distribution-based comparisons further demonstrated clear differences in the PAI value distributions between acquisition years. In 2014, there are generally more very-low-density values (see density plot where PAI < 2 in Figure 4c), while 2020 has more slightly higher PAI values. The distribution of the values in 2019 is different, with a larger number of low PAI values. Pairwise KS tests support this observation, and yielded large D statistics for all three methods, indicating limited overlap between the distributions. Across methods, the largest distributional differences were observed in comparisons involving the 2019 acquisition, while comparisons between 2014 and 2020 generally showed smaller D statistics. This pattern was consistent across all three PAI estimation methods, although the magnitude of the differences varied. Among the tested approaches,

https://doi.org/10.5194/egusphere-2026-1689
Preprint. Discussion started: 31 March 2026

AMAPVox exhibited the smallest distributional differences between 2014 and 2020. Detailed statistical results for all interannual comparisons are provided in the Supplementary Material.

The boxplots depicted in Figure 5 show the estimated PAI in the different forest types (coniferous, mixed coniferous, mixed deciduous and deciduous).

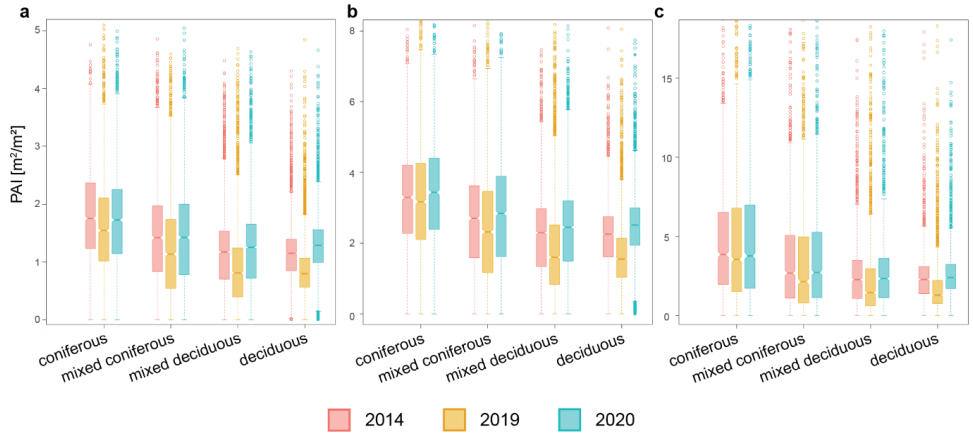

Figure 5: Boxplots of the plant area index (PAI) values in the different forest types, estimated using the methods leafR (a), Arnqvist (b) and AMAPVox (c). The PAI ranges are different for each method.

As expected, PAI was lower in more deciduous forest patches due to the leaf off condition during acquisition. Interannual variability increased with a higher proportion of deciduous trees, a pattern that was consistently reflected in the statistical comparison of pixel-wise PAI values across forest types (Tables S6-S8). In deciduous forests, lower PAI values were estimated with all methods in 2019, whereas PAI distributions from 2014 and 2020 were more similar. This behaviour was also evident in the statistical results, which showed larger median shifts and more pronounced distributional differences for deciduous and mixed deciduous forest classes than for coniferous forests.

In contrast, PAI values in coniferous forests were very similar across all three study years, particularly when the AMAPVox and Arnqvist methods were applied (Figure 5c). Correspondingly, statistical comparisons indicated small interannual median differences and a high similarity of PAI value distributions in coniferous stands. With increasing conifer dominance, the interannual consistency of PAI distributions increased, a trend that was also present for the leafR method, albeit less pronounced.

For a more detailed view of PAI value distributions across forest types, density plots derived from the Arnqvist method are shown in Figure 6. For comparison, the reference forest (see Sect. 2.2.2) was included in Figure 6e.

https://doi.org/10.5194/egusphere-2026-1689
Preprint. Discussion started: 31 March 2026

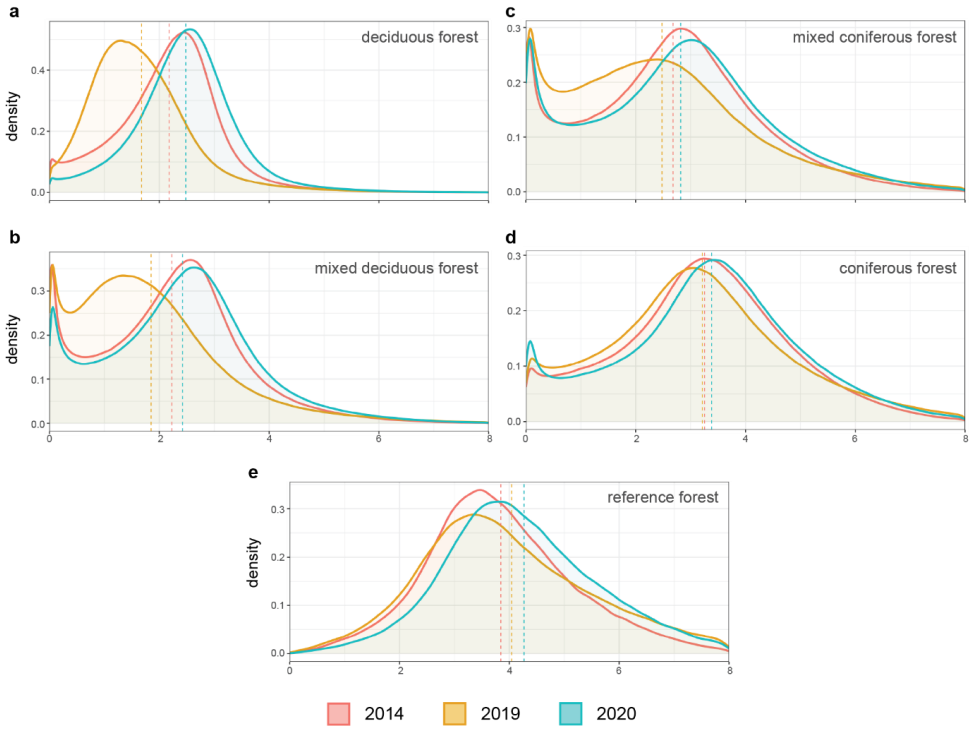

Figure 6: Density plots of the plant area index (PAI) values for all three study years in different forest types, estimated using the Arnqvist method. The considered forest types are deciduous (a), mixed deciduous (b), mixed coniferous (c), coniferous (d) and reference forest (e). The dashed vertical line in the density plots indicates the mean value.

The reference forest showed slightly higher apparent variability than the pure coniferous forest, which coincided with a substantially smaller number of valid pixel pairs and thus reduced spatial averaging (Tables S6-S8).

Influence of sensor parameters

To further investigate the observed variability in vegetation density metrics and assess the influence of acquisition parameters, we performed a detailed inspection of selected forest patches. We selected ten 20 × 20 m forest patches that were either deciduous- or coniferous-dominated, to investigate how vegetation density changes in the forest profile (two are shown in Figure 7). The echo density was lower in 2014 than in the other years, which affects the representation of tree structure. We saw that, especially in the deciduous forest patch, only few returns were measured below the canopy in 2014 (Figure 7b). As a result, the stems and lower parts of the trees lacked in detail. The highest level of detail below the canopy was seen in the data from 2019, which corresponds to the highest point density for this recording year. The difference was not as pronounced in the coniferous forest patch, where the point clouds of all three study years looked very similar.

https://doi.org/10.5194/egusphere-2026-1689
Preprint. Discussion started: 31 March 2026

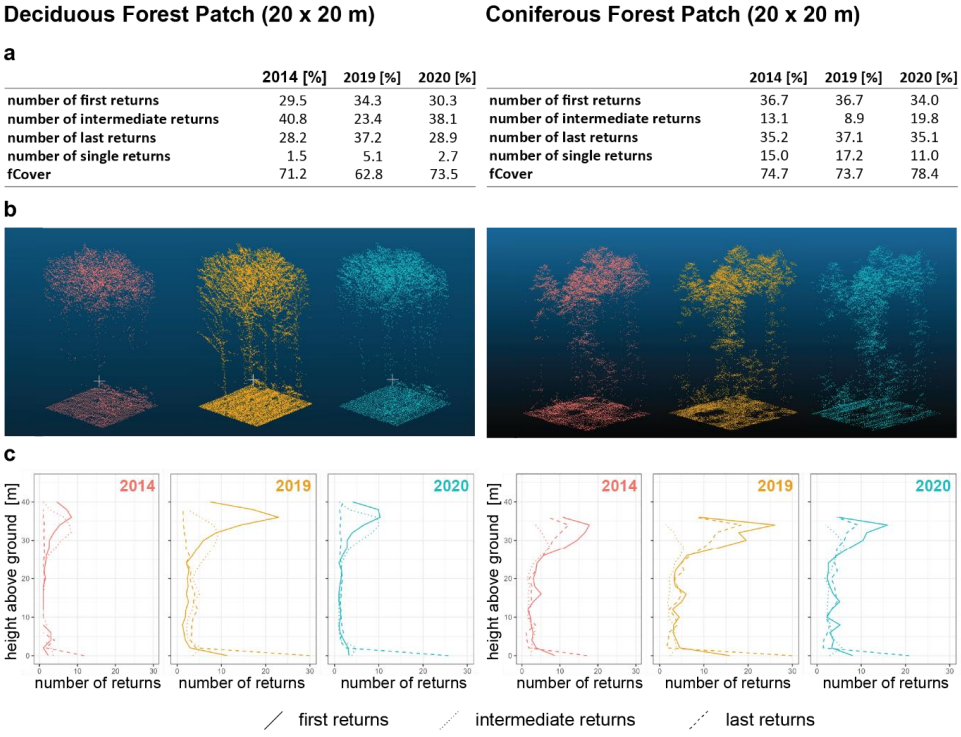

Deciduous Forest Patch (20 x 20 m)	2014 [%]	2019 [%]	2020 [%]
number of first returns	29.5	34.3	30.3
number of intermediate returns	40.8	23.4	38.1
number of last returns	28.2	37.2	28.9
number of single returns	1.5	5.1	2.7
fCover	71.2	62.8	73.5

Coniferous Forest Patch (20 x 20 m)	2014 [%]	2019 [%]	2020 [%]
number of first returns	36.7	36.7	34.0
number of intermediate returns	13.1	8.9	19.8
number of last returns	35.2	37.1	35.1
number of single returns	15.0	17.2	11.0
fCover	74.7	73.7	78.4

Figure 7: Details of a 20 × 20 m deciduous (left) and coniferous forest patch (right). The relative numbers of first, intermediate, last and single returns and the fractional cover (fCover; as in Morsdorf et al. (2006)) of all study years are depicted in a, the respective point clouds in b, and their distribution of the absolute number of returns over the height above ground in c.

In Figure 7, the ratio of the first, intermediate and last returns are printed together with their respective point clouds and distributions over the height above ground. There were more intermediate returns in 2014 and 2020 than in 2019, when the pulse repetition frequency (PRF) was significantly higher (Table 1). This effect was most noticeable in the deciduous forest patch, where the intermediate returns made up around 40% of all returns in 2014 and 2020 but only 23.4% in 2019. Furthermore, the fractional cover (fCover as in Morsdorf et al. (2006)) decreased much more between 2014 and 2019 in the deciduous forest patch than in the coniferous forest patch. In Figure 7c, the number of first returns peaked very close to the highest point of the canopy, followed by a peak of intermediate returns directly below. Although this pattern was the same for all study years, in 2019 the number of first returns was much greater than the number of intermediate returns, whereas the peak of the number of first and intermediate returns was similar in 2014 and 2020.

This was not visible in the coniferous forest patch. Although the proportion of the number of intermediate returns was still lower in 2019 (8.9%) compared with 2014 (13.1%) and 2020 (19.8%), they had a much lower impact compared with the first and last returns (Figure 7a). This was also evident in Figure 7c, where it was not the first and intermediate returns that peaked in the top canopy layer, but rather the first and last returns. While the intermediate returns still peaked slightly below the first returns, their contribution was much less pronounced.

https://doi.org/10.5194/egusphere-2026-1689
Preprint. Discussion started: 31 March 2026

4 Discussion

4.1 Scale sensitivity

Our sensitivity analysis of the influence of cell size on the estimated morphological traits showed that the larger the cell size, the less variation that can be measured in all traits with all methods. Larger cells average over more forest structure, which smooths out local extremes. This results in overall lower variation, higher estimated CH, and lower apparent PAI.

In our CH examination, there is no cell size that is evidently the best choice concerning the capture of variation in forest space. A small cell size (< 2 × 2 m) would still give good results and show more variation than larger sizes. CH can be measured accurately even with small cell sizes, as Fischer et al. (2024) used 1 × 1 m.

In the PAI estimations, the most variation can be captured with a cell size of 2 × 2 m, where the mean PAI values also are the highest. All methods seem to estimate lower PAI in smaller cell sizes (see Figure 2). Possible reasons for this phenomenon could be a lack of LiDAR returns in very small cells and thus the algorithms not performing accurately or occlusion leading to voxels without echoes, having large impact in small voxel sizes. We therefore decided to use the 2 × 2 m resolution for all the metrics and methods, to have consistent and comparable results.

The Arnqvist method is sensitive to grid size in heterogeneous forests (Arnqvist et al., 2020). Despite the sensitivity analysis, it is possible that the 2 × 2 m grid we applied might not have been appropriate in all areas of the study area and might have led to uncertainties. In areas with low point density, where the 2 × 2 m spatial resolution is too small for the number of available returns, larger uncertainties in estimated PAI can be expected. Without in-situ validation data, it was not possible to give exact numbers for such uncertainties. To mitigate this problem, one could filter out pixels with point densities below a certain threshold.

Overall, a cell size of 2 × 2 m offers a good compromise between spatial detail and data robustness. It is small enough to capture sub-canopy structural variation, such as parts of individual trees, while still ensuring that enough ALS returns fall within each cell to enable PAI estimation. This will obviously depend on the average point density of the ALS dataset. Although small cell sizes can potentially lead to noisy outputs, due to low point densities, we did not observe such artifacts in our data. As a result, no spatial averaging or smoothing was applied.

4.2 Differences in structural traits

To understand the change in the traits we considered, it is important to note that the input data we used originate from different providers and show large variation due to different scanning geometries and sensor specifications, as typically observed when analysing multi-temporal operational ALS data. These differences can influence the resulting traits and could lead to inconsistencies in the time series, as discussed in the following sub-sections.

4.2.1 General sensor and flight-setting effects on trait estimation methods

A commercial laser sensor has typically a relatively short life cycle of often fewer than 4 years. This leads to subsequent ALS data acquisitions usually being recorded with different instruments (Ørka et al., 2010). Differences in sensors and flight settings between ALS acquisitions substantially affect derived structural parameters, such as height and density (Morsdorf et al., 2008; Næsset, 2009; Ørka et al., 2010; Solberg et al., 2009).

Higher flying altitude has been related to a reduction of the peak pulse power concentration where the laser pulse hits the surface. This leads to lower backscatter intensities, which has implications for the estimated structural parameters (Hopkinson, 2007). The high flying altitude (> 1200 m) in 2019 and 2020 compared with in 2014 (600 m) can be partially compensated by the smaller beam divergence (0.25 mrad in 2019 and 2020 compared with 0.5 mrad in 2014), but it still results in lower

https://doi.org/10.5194/egusphere-2026-1689
Preprint. Discussion started: 31 March 2026

backscatter intensities. Therefore, some intermediate echoes have probably not been recorded due to their backscatter intensity being below the noise level and/or detection threshold (Korpela et al., 2012). A reduction in the peak pulse power concentration is also expected in the 2019 ALS dataset, due to the higher PRF (1000 kHz compared with 300 kHz in 2014) (White et al., 2016). This intensity reduction is associated with a decrease in recorded intermediate echoes and with increased canopy penetration before the first return because the reduced power of the laser pulse needs to travel further into the canopy until the backscatter intensity is high enough for the sensor to record a first return. These effects have been recognized, especially for tall vegetation with canopy gaps (Hopkinson, 2007). Our analysis was based on leaf-off datasets, implying a less dense canopy at the time of acquisition. Given that the study area is dominated by mixed and deciduous forest types, increased laser pulse penetration through the canopy is to be expected (Canton Aargau: Departement Bau Verkehr und Umwelt, 2018). Such effects are visible in our data, with the most pronounced effect occurring in our 2019 data, where the relative number of intermediate returns is much lower, especially in forests with more deciduous trees (Figure 7).

4.2.2 Height metrics

As we have shown in this study and as was also reported in other studies (Coops et al., 2016), CH can be robustly estimated from ALS data. The high robustness of CH estimates across acquisition years is supported by the very small interannual differences in central tendency and the near-identical value distributions observed in the statistical comparisons reaffirming also the suitability of the used operational ALS data. Thus, we can interpret the observed differences ecologically or from a forest management point of view.

We hypothesized that differences in mean CH over the entire study area between time steps would be close to zero, as localized increases and decreases are likely to balance each other out across a large and diverse study area. The observed decrease in mean CH is indeed small—from 21.44 m in 2014 to 21.26 m in 2020—and thus supports this hypothesis. This slight decline could be explained by forest management activities or cumulative abiotic stress (e.g. windthrow or drought), which may obscure expected growth signals in certain parts of the landscape.

Several hot and dry years occurred between the ALS acquisitions. 2015, 2017 and 2018 rank among the warmest years in Switzerland since the beginning of meteorological measurements in 1864 (MeteoSwiss, 2020; Sturm et al., 2022). These years were also characterized by low water availability. According to aridity index values published by the Swiss Federal Office for the Environment (FOEN), plants experienced considerable drought stress in these years, leading to reduced photosynthetic activity and increased vulnerability (Remund and Augustin, 2015). Such conditions could have contributed to local canopy decline or tree mortality, potentially explaining part of the observed decrease in CH. For a detailed analysis of regional drought impacts on Swiss forest ecosystems, we refer to Remund and Augustin (2015).

When examining the different CH classes, we found that area of patches with very tall vegetation (> 35 m) remained largely unchanged, while a slight decrease was observed in the 27–34 m height range between 2014 and 2020, supporting the observations described above. Very tall trees do not appear to be affected by this. Also, tree growth is not expected to influence these larger and thus probably older trees considerably, meaning that large differences are not expected in these CH ranges. We observed the largest changes below a CH of 20 m. This is reasonable, as tree growth and forest clearing are most dynamic in this height class.

With respect to the potential influence of reduced peak pulse power concentration, we did not observe clear effects in the 2019 dataset, where the PRF was substantially higher than in the other acquisition years.

CH is suitable for determining both large and small changes between years. As the observed height changes are the same for Hmax and H95, both metrics can be used for this purpose, depending on the application requirements. Still, the results using H95 are less noisy, more stable and less prone to outliers than Hmax, indicating that H95 is the better choice for most applications.

https://doi.org/10.5194/egusphere-2026-1689
Preprint. Discussion started: 31 March 2026

4.2.3 Density metrics

Compared with CH, PAI is much more sensitive to sensor and flight settings. This contrast between CH and PAI is not limited to visual differences in the maps and density plots but is consistently reflected in the statistical comparison of interannual variability across all tested PAI estimation methods. While we did not use independent height reference data to validate the CH estimates in this study, CH derived from ALS has been extensively validated in numerous previous studies and is widely considered robust and accurate. We therefore have high confidence in the precision and reliability of the CH estimates. In contrast, PAI estimates are hard to validate due to a lack of accurate reference values, as ground-based estimates also carry uncertainty (Arnqvist et al., 2020). Consequently, we cannot interpret temporal changes in PAI in the same way as CH, and instead need to investigate the influence of the sensor and flight parameters on our methods and trait results.

While PAI served as the focal trait in this study due to its ecological relevance, the implications extend well beyond this single metric. Other density- or percentile-based forest metrics, including many commonly used ALS-derived 3D structural variables or related voxel- and distribution-based approaches, are likely affected in a similar way. Thus, the challenges identified here are not specific to PAI but reflect a broader limitation in multitemporal ALS analyses of complex structural traits.

Influence of sensor parameters

The influence of scan angle and point density appears to be negligible, as the methods used here seem to compensate sufficiently for these factors, resulting in no or only minimal observable effects. This is supported by the fact that the results from 2014 and 2020 are very similar, despite differences in scan angle and variations in point density.

In contrast, the influence of PRF appears to be pronounced. A higher PRF reduces the energy per emitted pulse, meaning that weak echoes – typically from small reflective surfaces like fine branches or sparse vegetation – may not meet the sensor's return threshold, as described in Sect. 4.2.1. This is especially true in leafless conditions or in areas with lower vegetation density, where less energy is reflected, reducing the likelihood of capturing intermediate returns. This effect likely explains the larger discrepancies observed in the PAI of deciduous forest areas between the 2014/2020 and 2019 datasets. As a result, first and last returns dominate, with very few intermediate returns recorded. The observed decrease in fCover in 2019 over the deciduous forest patch, and the absence of such an effect in the coniferous stand, further illustrates this pattern. These return characteristics influence the PAI estimation, as methods like Arnqvist and AMAPVox weight returns based on their return number, while leafR does not differentiate between them. The weighting of returns in the Arnqvist and AMAPVox methods may partly explain the observed differences in PAI. In contrast, the effect of leafR's lack of differentiation between return numbers—in our implementation, all returns were effectively treated as first returns—remains unclear and would require further investigation to quantify its influence.

Overall, these findings suggest that PRF settings and their interaction with forest structure and phenology are critical factors influencing return distributions and subsequent canopy parameter estimation in our datasets. Shao et al. (2019) proposed a linear correction model to address sensor-related biases in tropical forests, but its applicability to our temperate, mixed forests under leaf-off conditions is limited due to fundamentally different phenology and forest structure. A universal correction approach is therefore unlikely to capture the observed variability. Further research is needed to systematically investigate these effects and refine methodological adjustments to improve result consistency across varying forest types and acquisition parameters.

Forest composition and PAI variability

In winter conditions (leaf-off in deciduous forests), evergreen coniferous forests typically exhibit higher vegetation density and a more closed canopy structure than deciduous forests, which appear more open due to the absence of foliage. This difference is clearly reflected in the PAI values across the forest types in our study (Figure 6).

https://doi.org/10.5194/egusphere-2026-1689
Preprint. Discussion started: 31 March 2026

Forest composition, specifically the proportion of deciduous and coniferous species, has a clear influence on the robustness of PAI estimations across years. As shown in Figure 6 and the statistical results (Tables S6-S8), interannual variation in vegetation density metrics is highest in deciduous stands and progressively decreases with increasing conifer dominance. In pure coniferous forests, PAI distributions are notably consistent across all three acquisition years, whereas deciduous-dominated forests exhibit marked differences, particularly in 2019.

These patterns align with the observations discussed in the previous section regarding the influence of acquisition parameters, especially PRF, on return characteristics. In deciduous forests under leaf-off conditions, fewer reflective surfaces below the canopy make PAI estimates more vulnerable to variations in return composition – an effect that is especially pronounced in the 2019 dataset. In contrast, the denser and more structurally stable canopies of coniferous stands are less affected by these acquisition differences, leading to more robust and consistent PAI values, even in 2019, when the dataset was acquired with a higher PRF than in the other years.

The reference forest, composed exclusively of mature coniferous trees, shows slightly higher PAI variability than expected. This can be attributed to the strict selection criteria for the reference forest, which resulted in fewer valid pixels and, consequently, increased sensitivity to local variation and outliers. Structurally stable, evergreen forests provide more consistent conditions for multitemporal trait analysis.

Overall, these findings underscore that forest type modulates the susceptibility of PAI metrics to acquisition-related variability. While coniferous forests yield robust and comparable density estimates, caution is warranted when interpreting multitemporal trends in mixed or deciduous stands without accounting for potential sensor-driven effects.

Considerations regarding seasonal influence

To conduct a multitemporal analysis, data acquired at a similar time of the year is needed to have all datasets either under leaf-on or leaf-off conditions. The fact that the canton of Aargau is dominated by deciduous tree species implies that we were only able to analyse woody material in a large part of the study area. Therefore, short-term changes in leaf composition due to disturbances before the ALS acquisitions did not influence the analysis. Additionally, density and layering of the lower canopy can be observed better, which would have been occluded in a summer ALS dataset. It has been recognized that leaf-off datasets are the next-best alternative after combined leaf-on and leaf-off data for such analyses because they enable a detailed characterization of the lower canopy layers (Davison et al., 2020).

Even though all the data used in this study are from leaf-off conditions, the recording dates were different in the individual study years (Table 1). In 2014 the acquisition dates were in March or early April, in 2019 the ALS recording took place in March or late April, and in 2020 it took place in early February or March. In **Error! Reference source not found.**, the mean air temperature and the beech leaf unfolding process in the time around the ALS acquisitions are depicted. The leaf unfolding in the forest started slightly earlier in 2014 than in 2019 and 2020. Although the ALS campaign in 2014 was later than that in 2020, the estimated PAI values are lower, indicating that small differences in phenology alone cannot explain the observed PAI variations and that acquisition parameters likely exert a stronger influence under leaf-off conditions.

https://doi.org/10.5194/egusphere-2026-1689
Preprint. Discussion started: 31 March 2026

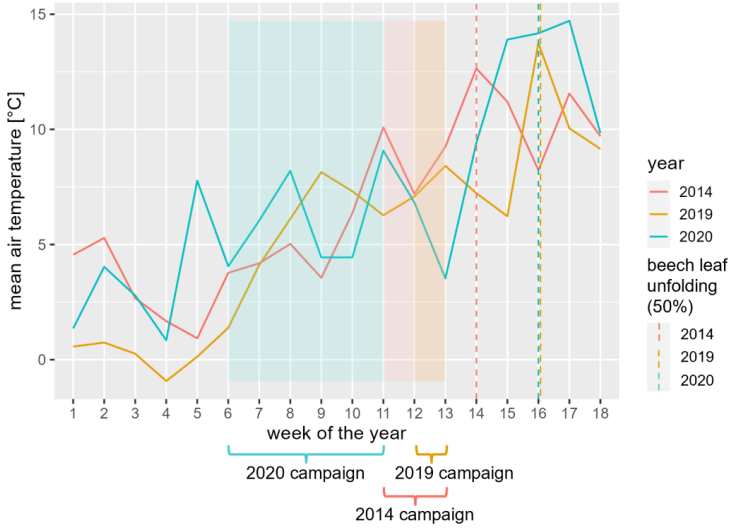

Figure 8: Mean air temperature before and during the ALS campaigns in 2014, 2019 and 2020, together with the 50% beech leaf unfolding (most frequent deciduous tree species in the test area). (MeteoSwiss, 2024)

Implications for method selection

All PAI retrieval methods rely on assumptions about the measurement system, yet they differ in how these assumptions propagate uncertainty into the results. Of the three methods tested in this study, the Arnqvist and AMAPVox approaches were more compatible with the characteristics of our operational ALS datasets, whereas the leafR method relies on assumptions that are difficult to fulfil under large-area acquisition settings.

Specifically, the leafR method would require scan angles close to nadir and first-return-only data. These conditions are rarely met in large-area, operational ALS acquisitions, where increased flying altitude and wider swath widths are commonly used to reduce acquisition costs by maximizing area coverage per flight line (Næsset, 2009). Restricting the analysis to first returns would furthermore have led to spatial gaps in our dataset, particularly in hilly terrain with limited flight strip overlap. We therefore applied the leafR method to all returns rather than only to first returns, as done by Arnqvist et al. (2020). This adaptation relaxes some of the original theoretical assumptions and thus introduces additional uncertainty, but it provides a computationally very inexpensive approach suitable for first-order approximations.

Although the leafR and Arnqvist approaches compute PAI as the vertical sum of PAD, they differ in handling zero transmission. LeafR replaces undefined layer-wise values (caused by zero `pulses.out`) with NA (= Not Available) and subsequent aggregation proceeds on the remaining valid layers, yielding finite PAI estimates. In the Arnqvist implementation, PAI estimation requires at least one ground-classified return within a raster cell, leading to many no-data gaps that can be observed in the maps where the ground is fully occluded (see example in Figure S2).

These differences directly affect the spatial patterns and value distributions observed in this study. Using the Arnqvist method, no-data gaps predominantly occur in high-density areas, indicating that PAI could not be retrieved for the densest forest stands. This likely leads to a systematic underestimation of high PAI values at the landscape scale. AMAPVox, by contrast, produced a wider PAI value range (Figure 4) and provided estimates in many of these dense areas, suggesting a better suitability under conditions of very dense forest stands.

The AMAPVox method delivers relatively stable values across years, especially when PRF settings are comparable, such as in the 2014 and 2020 datasets. However, this robustness comes at a cost: AMAPVox requires trajectory files, which are not always available and relies on a computationally intensive ray-tracing algorithm, which can demand substantial processing time and memory, particularly in mountainous terrain with large vertical voxel extents. Moreover, despite its detailed physical

https://doi.org/10.5194/egusphere-2026-1689
Preprint. Discussion started: 31 March 2026

modelling, the results remain sensitive to acquisition parameters affecting pulse energy density, such as PRF, beam divergence or flying altitude. At the same time, the large number of exposed parameters explicitly reflects the complexity of the ALS measurement system, and the assumptions required to model laser–vegetation interactions. This explicitness should not be seen as a disadvantage per se, as it highlights that PAI estimation is inherently complex and cannot be fully captured by simplified or implicit parameterizations.

Given these trade-offs, method selection should reflect the specific study objectives, data availability and acceptable balance between result precision and computational demands. For large study areas, rapid assessments or operational applications with limited metadata, simpler methods such as leafR or Arnqvist may be preferable. Despite its simple design, the leafR method provides quick and computationally inexpensive PAI results. This makes it suitable for gaining a rough overview or for preliminary analyses where immediate results are required. The Arnqvist method offers a middle ground: it provides fast and quite accurate results with substantially lower computational effort than AMAPVox and without the need for additional input data, making it well suited for many operational applications—especially because trajectory information is often unavailable. In contrast, AMAPVox may be more appropriate for high-detail investigations with abundant resources and comprehensive input data and where dense-canopy retrieval is of primary interest.

https://doi.org/10.5194/egusphere-2026-1689
Preprint. Discussion started: 31 March 2026

5 Conclusions

This study set out to evaluate the reliability and limitations of multitemporal forest trait analysis using operational ALS data, with CH serving as a baseline metric and PAI as a representative example of a complex, density-based structural trait.

While CH was confirmed to be a robust and reliable metric for multitemporal analyses, making it possible to analyse the results ecologically, more complex structural parameters like PAI proved particularly sensitive to variations in sensor and acquisition geometry. As a result, they cannot be interpreted as reliably as CH. Distinguishing real structural changes from external influences remains a persistent challenge, as varying acquisition parameters can lead to misinterpretations. Higher PRF reduces the energy per emitted pulse, which in turn lowers the resulting backscatter intensity. This can lead to fewer recorded intermediate returns, especially in deciduous forests, thereby limiting the vertical structural information captured by the sensor and introducing inconsistencies in density-based metrics such as PAI.

Importantly, the observed interannual differences cannot be attributed to a single factor. While PRF emerged as a particularly influential driver for our data, it is the interaction of multiple factors—including beam divergence, flying altitude, sensor-specific receiver characteristics, estimation method and forest type—that ultimately shapes ALS return distributions and propagates into PAI estimates. PRF therefore acts as a useful proxy for pulse characteristics in our case, but it should not be interpreted as the sole or universal cause of observed discrepancies. Furthermore, PAI represents only one example; the observed acquisition-related sensitivities are likely inherent to ALS-derived 3D structural variables in general.

None of the tested PAI estimation approaches yielded temporally consistent results across all acquisition years. This suggests that acquisition-related variability represents a fundamental limitation of multitemporal ALS analyses of density-based forest metrics when using operational datasets.

Still, methodological consistency is crucial in multitemporal analyses, as changes in the approach used to derive vegetation density can alter the value range of the results, thereby compromising the comparability of time series data. The choice of the PAI estimation method plays a crucial role in balancing accuracy, computational efficiency and data availability. Complex trait derivations from ALS data should thus be treated as relative rather than absolute measurements.

In this context, the choice of method may not be as critical as developing robust calibration approaches. Drawing from practices in optical remote sensing, future studies might benefit more from consistent calibration protocols than from the continuous refinement of structural metric approaches. Furthermore, identifying and standardizing acquisition parameters that drive metric deviations could enhance the stability of temporal analyses. Maintaining consistency in parameters that control laser pulse characteristics could foster more reliable and comparable ALS-based time series. While the use of identical sensors and harmonized acquisition parameters would simplify comparability, this is rarely feasible in practice due to the short life cycles of commercial sensors and the realities of large-scale mapping programs. Consequently, multitemporal analyses based on operational ALS data must accept a certain level of irreducible uncertainty.

Ultimately, understanding and mitigating acquisition-related variability is crucial for reliable multitemporal forest structure analysis with operational ALS. While refining structural metrics remains important, future progress may hinge on systematic data harmonisation efforts, as well as the development of calibration frameworks and acquisition standards that promote comparability across time and space.

https://doi.org/10.5194/egusphere-2026-1689
Preprint. Discussion started: 31 March 2026

Data availability

Point cloud data from 2014 and 2019 (canton of Aargau) are available at https://www.ag.ch/de/themen/staat-politik/daten-und-zahlen/geoportal/geodaten/geodatenliste and data from 2020 (SwissSURFACE3D) are available at https://www.swisstopo.admin.ch/de/hoehenmodell-swisssurface3d

Author contribution

Charis Moana Gretler: Conceptualization, Methodology, Formal analysis, Software, Validation, Investigation, Data Curation, Writing – Original Draft, Writing – Review & Editing, Visualization. **Daniel Kükenbrink:** Conceptualization, Methodology, Writing – Review & Editing. **Mauro Marty:** Methodology, Software, Data curation, Resources, Writing – Review & Editing. **Christian Ginzler:** Conceptualization, Methodology, Writing – Review & Editing, Project administration, Supervision, Funding acquisition. **Felix Morsdorf:** Conceptualization, Methodology, Supervision, Writing – Review & Editing.

Competing interests

The authors declare that they have no conflict of interest.

Acknowledgements

This study was carried out in the framework of the Swiss National Forest Inventory (NFI), a cooperative effort between the Swiss Federal Institute for Forest, Snow and Landscape Research (WSL) and the Swiss Federal Office for the Environment (FOEN). We thank Melissa Dawes for proofreading the manuscript.

Software to convert .las data to PAI using the Arnqvist method was provided by J, Arnqvist, and is available at URL: https://github.com/johanarnqvist/ALS2PAD.git.

During the preparation of this work the authors used OpenAI's ChatGPT 5 in order to improve the clarity and language of the text. After using this tool, the authors reviewed and edited the content as needed and take full responsibility for the content of the publication.

https://doi.org/10.5194/egusphere-2026-1689
Preprint. Discussion started: 31 March 2026

References

de Almeida, D. R. A., Stark, S. C., Shao, G., Schietti, J., Nelson, B. W., Silva, C. A., Gorgens, E. B., Valbuena, R., Papa, D. de A., and Brancalion, P. H. S.: Optimizing the remote detection of tropical rainforest structure with airborne lidar: Leaf area profile sensitivity to pulse density and spatial sampling, Remote Sens. (Basel)., 11, https://doi.org/10.3390/rs11010092, 2019.

de Almeida, D. R. A., Stark, S. C., Silva, C. A., Hamamura, C., and Valbuena, R.: leafR: Calculates the Leaf Area Index (LAD) and Other Related Functions, 2022.

Arnqvist, J., Freier, J., and Dellwik, E.: Robust processing of airborne laser scans to plant area density profiles, Biogeosciences, 17, 5939–5952, https://doi.org/10.5194/bg-17-5939-2020, 2020.

Arumäe, T., Lang, M., and Laarmann, D.: Thinning- and tree-growth-caused changes in canopy cover and stand height and their estimation using low-density bitemporal airborne lidar measurements – a case study in hemi-boreal forests, Eur. J. Remote Sens., 53, 113–123, https://doi.org/10.1080/22797254.2020.1734969, 2020.

Bojinski, S., Verstraete, M., Peterson, T. C., Richter, C., Simmons, A., and Zemp, M.: The concept of essential climate variables in support of climate research, applications, and policy, Bull. Am. Meteorol. Soc., 95, 1431–1443, https://doi.org/10.1175/BAMS-D-13-00047.1, 2014.

Bonan, G. B.: Forests and climate change: Forcings, feedbacks, and the climate benefits of forests, Science (1979)., 320, 1444–1449, https://doi.org/https://doi.org/10.1126/science.1155121, 2008.

Brändli, U.-B., Abegg, M., and Allgaier Leuch, B.: Schweizerisches Landesforstinventar. Ergebnisse der vierten Erhebung 2009–2017., 2020.

Canton Aargau: Departement Bau Verkehr und Umwelt: Zustand und Entwicklung des Aargauer Waldes: Ergebnisse der 2. Aargauer Waldinventur 2016, 2018.

Chen, J. M., Black, T. A., and Adams, R. S.: Evaluation of hemispherical photography for determining plant area index and geometry of a forest stand, Agric. For. Meteorol., 56, 129–143, https://doi.org/10.1016/0168-1923(91)90108-3, 1991.

Coops, N. C., Tompaski, P., Nijland, W., Rickbeil, G. J. M., Nielsen, S. E., Bater, C. W., and Stadt, J. J.: A forest structure habitat index based on airborne laser scanning data, Ecol. Indic., 67, 346–357, https://doi.org/10.1016/j.ecolind.2016.02.057, 2016.

Davison, S., Donoghue, D. N. M., and Galiatsatos, N.: The effect of leaf-on and leaf-off forest canopy conditions on LiDAR derived estimations of forest structural diversity, Int. J. Appl. Earth Obs. Geoinf., 92, 102160, https://doi.org/10.1016/j.jag.2020.102160, 2020.

Fahey, R. T., Atkins, J. W., Gough, C. M., Hardiman, B. S., Nave, L. E., Tallant, J. M., Nadehoffer, K. J., Vogel, C., Scheuermann, C. M., Stuart-Haëntjens, E., Haber, L. T., Fotis, A. T., Ricart, R., and Curtis, P. S.: Defining a spectrum of integrative trait-based vegetation canopy structural types, Ecol. Lett., 22, 2049–2059, https://doi.org/10.1111/ele.13388, 2019.

Federal Office of Topography swisstopo: swissBOUNDARIES3D, 2022.

Fischer, F. J., Jackson, T., Vincent, G., and Jucker, T.: Robust characterisation of forest structure from airborne laser scanning — a systematic assessment and sample workflow for ecologists, Methods Ecol. Evol., https://doi.org/10.1111/2041-210X.14416, 2024.

Helfenstein, I. S., Schneider, F. D., Schaepman, M. E., and Morsdorf, F.: Assessing biodiversity from space: Impact of spatial and spectral resolution on trait-based functional diversity, Remote Sens. Environ., 275, 113024, https://doi.org/10.1016/j.rse.2022.113024, 2022.

Homolová, L., Malenovský, Z., Clevers, J. G. P. W., García-Santos, G., and Schaepman, M. E.: Review of optical-based remote sensing for plant trait mapping, Ecological Complexity, 15, 1–16, https://doi.org/10.1016/j.ecocom.2013.06.003, 2013.

Hopkinson, C.: The influence of flying altitude, beam divergence, and pulse repetition frequency on laser pulse return intensity and canopy frequency distribution, Canadian Journal of Remote Sensing, 33, 312–324, https://doi.org/10.5589/m07-029, 2007.

https://doi.org/10.5194/egusphere-2026-1689
Preprint. Discussion started: 31 March 2026

Hopkinson, C. and Chasmer, L.: Testing LiDAR models of fractional cover across multiple forest ecozones, Remote Sens. Environ., 113, 275–288, https://doi.org/10.1016/j.rse.2008.09.012, 2009.

Hyyppä, J., Hyyppä, H., Leckie, D., Gougeon, F., Yu, X., and Maltamo, M.: Review of methods of small-footprint airborne laser scanning for extracting forest inventory data in boreal forests, Int. J. Remote Sens., 29, 1339–1366, https://doi.org/10.1080/01431160701736489, 2008.

Isenburg, M.: LAStools — Efficient tools for LiDAR processing., http://rapidlasso.com/LAStools, 2022.

Ishii, H. T., Tanabe, S. I., and Hiura, T.: Exploring the relationships among canopy structure, stand productivity, and biodiversity of temperate forest ecosystems, Forest Science, 50, 342–355, 2004.

Korpela, I., Hovi, A., and Morsdorf, F.: Understory trees in airborne LiDAR data – selective mapping due to transmission losses and echo-triggering mechanisms, Remote Sens. Environ., 119, 92–104, https://doi.org/10.1016/j.rse.2011.12.011, 2012.

Kozniewski, M., Kolendo, Ł., Ksepko, M., and Chmur, S.: Tracking Individual Scots Pine (Pinus sylvestris L.) Height Growth Using Multi-Temporal ALS Data from North-Eastern Poland, Remote Sens. (Basel)., 14, https://doi.org/10.3390/rs14174170, 2022.

Leiterer, R., Furrer, R., Schaepman, M. E., and Morsdorf, F.: Retrieval of canopy structure types for forest characterization using multi-temporal airborne laser scanning, in: IEEE International Geoscience & Remote Sensing Symposium, 2650–2653, 2015a.

Leiterer, R., Torabzadeh, H., Furrer, R., Schaepman, M. E., and Morsdorf, F.: Towards automated characterization of canopy layering in mixed temperate forests using airborne laser scanning, Forests, 6, 4146–4167, https://doi.org/10.3390/f6114146, 2015b.

Liu, J., Li, L., Akerblom, M., Wang, T., Skidmore, A., Zhu, X., and Heurich, M.: Comparative evaluation of algorithms for leaf area index estimation from digital hemispherical photography through virtual forests, Remote Sens. (Basel)., 13, 1–25, https://doi.org/10.3390/rs13163325, 2021.

McElhinny, C., Gibbons, P., Brack, C., and Bauhus, J.: Forest and woodland stand structural complexity: Its definition and measurement, For. Ecol. Manage., 218, 1–24, https://doi.org/10.1016/j.foreco.2005.08.034, 2005.

MeteoSwiss: Klimareport 2019, Zürich, 96 pp., 2020.

MeteoSwiss: Phenological and meteorological observations, https://opendata.swiss/de/dataset/phanologische-beobachtungen/resource/fc79554f-ae06-4294-8f79-fa198483aa66, 2024.

Moles, A. T., Warton, D. I., Warman, L., Swenson, N. G., Laffan, S. W., Zanne, A. E., Pitman, A., Hemmings, F. A., and Leishman, M. R.: Global patterns in plant height, Journal of Ecology, 97, 923–932, https://doi.org/10.1111/j.1365-2745.2009.01526.x, 2009.

Morsdorf, F., Kötz, B., Meier, E., Itten, K. I., and Allgöwer, B.: Estimation of LAI and fractional cover from small footprint airborne laser scanning data based on gap fraction, Remote Sens. Environ., 104, 50–61, https://doi.org/10.1016/j.rse.2006.04.019, 2006.

Morsdorf, F., Frey, O., Meier, E., Itten, K. I., and Allgöwer, B.: Assessment of the influence of flying altitude and scan angle on biophysical vegetation products derived from airborne laser scanning, Int. J. Remote Sens., 29, 1387–1406, https://doi.org/10.1080/01431160701736349, 2008.

Næsset, E.: Effects of different sensors, flying altitudes, and pulse repetition frequencies on forest canopy metrics and biophysical stand properties derived from small-footprint airborne laser data, Remote Sens. Environ., 113, 148–159, https://doi.org/10.1016/j.rse.2008.09.001, 2009.

Noss, R. F.: Indicators for Monitoring Biodiversity: A Hierarchical Approach, Conservation Biology, 4, 355–364, https://doi.org/10.1111/j.1523-1739.1990.tb00309.x, 1990.

https://doi.org/10.5194/egusphere-2026-1689
Preprint. Discussion started: 31 March 2026

Ørka, H. O., Næsset, E., and Bollandsås, O. M.: Effects of different sensors and leaf-on and leaf-off canopy conditions on echo distributions and individual tree properties derived from airborne laser scanning, Remote Sens. Environ., 114, 1445–1461, https://doi.org/10.1016/j.rse.2010.01.024, 2010.

Pearse, G. D., Watt, M. S., Dash, J. P., Stone, C., and Caccamo, G.: Comparison of models describing forest inventory attributes using standard and voxel-based lidar predictors across a range of pulse densities, International Journal of Applied Earth Observation and Geoinformation, 78, 341–351, https://doi.org/10.1016/j.jag.2018.10.008, 2019.

Remund, J. and Augustin, S.: Zustand und Entwicklung der Trockenheit in Schweizer Wäldern, Schweizerische Zeitschrift fur Forstwesen, 166, 352–360, https://doi.org/10.3188/szf.2015.0352, 2015.

Riofrío, J., White, J. C., Tompalski, P., Coops, N. C., and Wulder, M. A.: Harmonizing multi-temporal airborne laser scanning point clouds to derive periodic annual height increments in temperate mixedwood forests, Canadian Journal of Forest Research, 52, 1334–1352, https://doi.org/10.1139/cjfr-2022-0055, 2022.

Schneider, F. D., Morsdorf, F., Schmid, B., Petchey, O. L., Hueni, A., Schimel, D. S., and Schaepman, M. E.: Mapping functional diversity from remotely sensed morphological and physiological forest traits, Nat. Commun., 8, 1–12, https://doi.org/10.1038/s41467-017-01530-3, 2017.

Shao, G., Stark, S. C., de Almeida, D. R. A., and Smith, M. N.: Towards high throughput assessment of canopy dynamics: The estimation of leaf area structure in Amazonian forests with multitemporal multi-sensor airborne lidar, Remote Sens. Environ., 221, 1–13, https://doi.org/10.1016/j.rse.2018.10.035, 2019.

Skidmore, A. K., Pettorelli, N., Coops, N. C., Geller, G. N., Hansen, M., Lucas, R., Mücher, C. A., O'Connor, B., Paganini, M., Pereira, H. M., Schaepman, M. E., Turner, W., Wang, T., and Wegmann, M.: Environmental science: Agree on biodiversity metrics to track from space, Nature, 523, 403–405, https://doi.org/10.1038/523403a, 2015.

Solberg, S., Brunner, A., Hanssen, K. H., Lange, H., Næsset, E., Rautiainen, M., and Stenberg, P.: Mapping LAI in a Norway spruce forest using airborne laser scanning, Remote Sens. Environ., 113, 2317–2327, https://doi.org/10.1016/j.rse.2009.06.010, 2009.

Stahl, U., Reu, B., and Wirth, C.: Predicting species' range limits from functional traits for the tree flora of North America, Proc. Natl. Acad. Sci. U. S. A., 111, 13739–13744, https://doi.org/10.1073/pnas.1300673111, 2014.

Sturm, J., Santos, M. J., Schmid, B., and Damm, A.: Satellite data reveal differential responses of Swiss forests to unprecedented 2018 drought, Glob. Chang. Biol., 28, 2956–2978, https://doi.org/10.1111/gcb.16136, 2022.

Tompalski, P., White, J. C., Coops, N. C., and Wulder, M. A.: Demonstrating the transferability of forest inventory attribute models derived using airborne laser scanning data, Remote Sens. Environ., 227, 110–124, https://doi.org/10.1016/j.rse.2019.04.006, 2019.

Tymińska-Czabańska, L., Hawryło, P., and Socha, J.: Assessment of the effect of stand density on the height growth of Scots pine using repeated ALS data, International Journal of Applied Earth Observation and Geoinformation, 108, https://doi.org/10.1016/j.jag.2022.102763, 2022.

Vincent, G., Antin, C., Laurans, M., Heurtebize, J., Durrieu, S., Lavalley, C., and Dauzat, J.: Mapping plant area index of tropical evergreen forest by airborne laser scanning. A cross-validation study using LAI2200 optical sensor, Remote Sens. Environ., 198, 254–266, https://doi.org/10.1016/j.rse.2017.05.034, 2017.

Vincent, G., Pimont, F., and Verley, P.: Various PAD / LAD estimators implemented in AMAPVox 1.8.0, 2–6, 2021.

Waser, L. and Ginzler, C.: Forest Type NFI, https://doi.org/10.16904/1000001.3, 2021.

White, J. C., Coops, N. C., Wulder, M. A., Vastaranta, M., Hilker, T., and Tompalski, P.: Remote Sensing Technologies for Enhancing Forest Inventories: A Review, https://doi.org/10.1080/07038992.2016.1207484, 2 September 2016.

Wilkes, P., Jones, S. D., Suarez, L., Haywood, A., Woodgate, W., Soto-Berelov, M., Mellor, A., and Skidmore, A. K.: Understanding the effects of ALS pulse density for metric retrieval across diverse forest types, Photogramm. Eng. Remote Sensing, 81, 625–635, https://doi.org/10.14358/PERS.81.8.625, 2015.

https://doi.org/10.5194/egusphere-2026-1689
Preprint. Discussion started: 31 March 2026

Zheng, Z., Zeng, Y., Schneider, F. D., Zhao, Y., Zhao, D., Schmid, B., Schaepman, M. E., and Morsdorf, F.: Mapping functional diversity using individual tree-based morphological and physiological traits in a subtropical forest, Remote Sens. Environ., 252, https://doi.org/10.1016/j.rse.2020.112170, 2021.

760